

Research Report

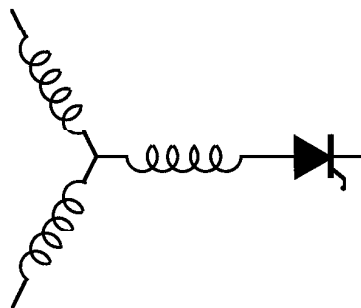
**97-30**

**Analysis and Evaluation of the Transverse Flux  
Circumferential Current Machine**

**S. Huang\*, J. Luo, T.A. Lipo**

Wisconsin Power Electronics  
Research Center  
University of Wisconsin-Madison  
Madison WI 53706-1691

\* College of Automation  
Shanghai University  
147 Yan-Chang Road  
Shanghai, 200072, P.R. China



**Wisconsin  
Electric  
Machines &  
Power  
Electronics  
Consortium**

University of Wisconsin-Madison  
College of Engineering  
Wisconsin Power Electronics Research Center  
2559D Engineering Hall  
1415 Engineering Drive  
Madison WI 53706-1691

# Analysis and Evaluation of the Transverse Flux Circumferential Current Machine

Surong Huang\*

\*College of Automation  
Shanghai University  
147 Yan-Chang Road  
Shanghai, 200072, P. R. China

Jian Luo

Student Member, IEEE  
Department of Electrical & Computer Eng.  
University of Wisconsin-Madison  
1415 Engineering Drive  
Madison, WI 53706-1691, U.S.A.

Thomas A. Lipo

Fellow, IEEE

**Abstract** – With the evolution of novel high power density machines, it becomes important to compare the power potential of such machines with vastly different topologies having a variety of different waveforms of back emf and current. The approach of this paper is based on general-purpose sizing and power density equations, which will permit a comparison of the main dimensions and power of such machines. In this paper, the comparison method of machine power densities is extended to include the Transverse Flux Circumferential Current type permanent magnet (TFCCPM) machine, and furthermore to compare the power production capability between the TFCCPM machine and the well-known squirrel cage induction machine.

## I. INTRODUCTION

Traditional design of AC electrical machines is based on the premise that the machine has a cylindrical shape with radially directed air-gap flux and a single stator and rotor supplied by a sinusoidal source which assumes a sinusoidal emf at the air-gap of the machine. It was recognized in [1] and [2], however that the emergence of power electronic has removed the need for such a concept as the basis for machine design. Beginning with the switched reluctance machine, a new perspective of electrical machine design is evolving based on the principle that the best machine design is the one that simply produces the optimum match between the machine and the power electronic converter, the converter fed machine (CFM) [1].

The logical structure of a CFM system is idealized in Fig. 1. In order to study or compare among such systems, three types of analysis tools need be implemented; (1) a sizing analysis and optimization method for such electrical machines; (2) a convenient interface definition between the two objects of Fig. 1; (3) sizing and cost analysis of the associated converter. Although a practical optimized synthesis of a CFM can be developed only after these three tools are available, the sizing analysis, an optimization and

comparison, as well as the definition of the interface are the first main steps in such an approach and is the topic of this paper. As long as the models of electrical machines and the interface are clearly defined and studied, a design of a CFM can then be easily predicted based on a balanced selection between the converter rating (cost) and machine performance.

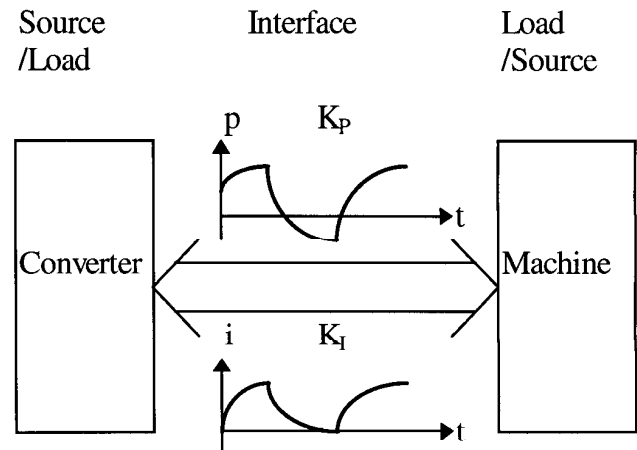


Fig. 1 A CFM system

In general, comparison of different machine types is a very formidable task. Only recently, in 1996, S. Huang et. al. [4] developed general-purpose sizing and power density equations and established a systematic method to compare the capabilities of machines with greatly different topologies. The procedure includes (1) a concept for comparing the power density on the basis of total occupied volume instead of air-gap volume; (2) special factors which were introduced to account for the effects of current and back emf waveforms. These factors also serve as a convenient interface definition for quantities related to both the converter and electrical machine; (3) comparison methods which were focused on radial flux and axial flux type machines respectively in [4] and [5].

As developments have occurred in the field of transverse flux PM machines, issues have been raised concerning the power density of unconventional machines when compared with more conventional topologies [3]. In this paper, as a further contribution to this study, a detailed approach will be presented for the application of the general-purpose sizing and power density equations to the TFCCPM machine, followed by a comparison of the TFCCPM machine with traditional induction machines.

## II. SIZING EQUATIONS AND POWER DENSITIES

Derived in Ref. [4], the general purpose sizing equations take the form,

$$P_R = \frac{1}{1+K_\phi} \frac{m}{m_1} \frac{\pi}{2} K_e K_i K_p \eta B_g A \frac{f}{p} \lambda_o^2 D_o^2 L_e \quad (1)$$

Or

$$P_R = \frac{1}{1+K_\phi} \frac{m}{m_1} \frac{\pi}{2} K_e K_i K_p K_L \eta B_g A \frac{f}{p} \lambda_o^3 D_o^3 \quad (2)$$

where,

- $P_R$  rated output power of the machine.
- $K_\phi$  ratio of electrical loading on rotor and stator.  
(In a machine without a rotor winding,  $K_\phi=0$ .)
- $m$  number of phases of the machine.
- $m_1$  number of phases of each stator (if there is more than one stator, each stator has the same  $m_1$ ).
- $K_e$  emf factor which incorporates the winding distribution factor  $K_w$  and the per unit portion of the total air gap area spanned by the salient poles of the machine (if any).
- $K_i$  current waveform factor.
- $K_p$  electrical power waveform factor.
- $\eta$  machine efficiency.
- $B_g$  flux density in the air-gap.
- $A$  total electrical loading includes both the stator electrical loading  $A_s$  and rotor electrical loading  $A_r$ .
- $f$  converter frequency.
- $p$  machine pole pairs.
- $D_o$  diameter of the outer surface of the machine.
- $L_e$  effective stack length of the machine.
- $K_L$  aspect ratio coefficient of the effective stack length vs. the diameter of the air-gap surface in radial air gap flux machines.
- $\lambda_o$  ratio of the diameter of the air-gap surface vs. the diameter of the outer surface of the machine.

In order to study the suitability of using the above general parameters for transverse flux machines, it is useful to consider the power production of this machine in detail. In general, if stator leakage inductance and resistance are

neglected, the output power for any electrical machine can be expressed as [4],

$$P_R = \eta \frac{m}{T} \int_0^T e(t) i(t) dt = \eta m K_p E_{pk} I_{pk} \quad (3)$$

where  $m$  is the phase number, and the emf  $e(t)$  and  $E_{pk}$  are the phase air-gap emf and its peak value. The currents  $i(t)$  and  $I_{pk}$  are the phase current and the peak phase current, and  $T$  is the period of one cycle of the emf. The factor  $K_p$  is defined as

$$K_p = \frac{1}{T} \int_0^T \frac{e(t) \times i(t)}{E_{pk} \times I_{pk}} dt = \frac{1}{T} \int_0^T f_e(t) f_i(t) dt \quad (4)$$

where  $f_e(t) = e(t)/E_{pk}$  and  $f_i(t) = i(t)/I_{pk}$  are the expressions for the normalized emf and current waveforms.

The emf in Eq. (3) for the transverse flux machines is given by

$$e(t) = \frac{d\Lambda_g(t)}{dt} = K_e N_t B_g \frac{f}{p} D_g L_e f_e(t) \quad (5)$$

where  $\Lambda_g$  is the air-gap flux linkage per phase,  $N_t$  is the number of turns per phase,  $D_g$  is the equivalent diameter of air-gap surface. From Eq. (5) it is apparent that

$$E_{pk} = K_e N_t B_g \frac{f}{p} D_g L_e \quad (6)$$

The current waveform factor  $K_i$  is defined in Ref. [4] as

$$K_i = \frac{I_{pk}}{I_{rms}} = \left( \frac{1}{T} \int_0^T \left( \frac{i(t)}{I_{pk}} \right)^2 dt \right)^{-1/2} \quad (7)$$

where  $I_{rms}$  is the rms phase current which is related to the stator electrical loading  $A_s$ . Due to the structure of transverse flux machines, there are double sided stator and air-gap surfaces in the radial direction. Hence, the stator electrical loading  $A_s$  includes both the electrical loading of outer stator winding  $A_{so}$  and the electrical loading of inner stator winding  $A_{si}$ , as shown in Eq. (8)

$$A_s = A_{si} + A_{so} = 2 N_t \frac{I_{rms}}{L_e} \quad (8)$$

In the general case, the total electrical loading  $A$  should include both the stator electrical loading  $A_s$  and rotor electrical loading  $A_r$ , so that, again from Ref. [4],

$$A_s = A - A_r = \frac{A}{1 + K_\phi} \quad (9)$$

From Eqs. (7), (8), and (9) an expression for the peak current can be found

$$I_{pk} = \frac{1}{1 + K_\phi} K_i A \frac{L_e}{2N_t} \quad (10)$$

Combining Eqs. (3), (6), (10), the  $L_e^2 D_g$  sizing equation for the transverse flux machines takes the form,

$$P_R = \frac{m}{2} \frac{1}{1 + K_\phi} K_e K_i K_p \eta B_g A \frac{f}{p} L_e^2 D_g \quad (11)$$

The aspect ratio coefficient is typically defined as [4]

$$K_L = \frac{L_e}{D_g} \quad (12)$$

This ratio should be selected based upon the practical requirements of the application. Inserting Eq. (12) into (11), it is possible to obtain the following  $D_g^3$  sizing equation

$$P_R = \frac{m}{2} \frac{1}{1 + K_\phi} K_e K_i K_p K_L^2 \eta B_g A \frac{f}{p} D_g^3 \quad (13)$$

To realize the  $D_o^2 L_e$  relationship necessary for sizing, it is useful to define the ratio [4]

$$\lambda_o = \frac{D_g}{D_o} = f(d_{sso}, d_{cso}, H_{pm}, D_g, p) \quad (14)$$

where  $d_{sso}$  is the depth of the outer stator slot,  $d_{cso}$  is the depth of the outer stator core and  $H_{pm}$  is the radial height of the permanent magnet in the rotor. In general, a procedure needs to be developed to determine  $\lambda_o$  when studying a specific machine or structure, which incorporates the effects of temperature rise, losses, and efficiency requirements on the design. In practice, the depths  $d_{sso}$ , and  $d_{cso}$  depend upon the stator electrical loading  $A_s$ , the current density  $J_s$ , the slot fill factor  $K_{cu}$  and the flux density in the iron core. The radial height  $H_{pm}$  depends on the flux focusing factor  $K_{focus}$  and pole pairs. The equivalent diameter of air-gap surface  $D_g$  is determined by Eq. (13).

TABLE I  
TYPICAL PROTOTYPE WAVEFORMS

Model	e(t)	i(t)	$K_i$	$K_p$
Sinusoidal waveform			$\sqrt{2}$	$\frac{1}{2} \cos \phi_r$
Sinusoidal waveform			$\sqrt{2}$	0.5
Rectangular waveform			1	1
Trapezoidal waveform			1.134	0.777
Triangular waveform			$\sqrt{3}$	0.333
Rectangular & Trapezoidal waveform			1.134	0.8
Rectangular & Trapezoidal waveform			1.389	0.556
Trapezoidal waveform			1.389	0.519
Rectangular & Trapezoidal waveform			1.5	0.333
Rectangular waveform			1.225	0.667

The final general purpose sizing equation ultimately takes on the form

$$P_R = \frac{m}{2} \frac{1}{1 + K_\phi} K_e K_i K_p K_L \eta B_g A \frac{f}{p} \lambda_o^2 D_o^2 L_e \quad (15)$$

For convenience in design and for purpose of comparison the corresponding  $D_o^3$  sizing equation can be found to be

$$P_R = \frac{m}{2} \frac{1}{1 + K_\phi} K_e K_i K_p K_L^2 \eta B_g A \frac{f}{p} \lambda_o^3 D_o^3 \quad (16)$$

The transverse flux machine power density for the total volume can now finally be defined as

$$\xi = \frac{P_R}{\frac{\pi}{4} D_o^2 L_e} \quad (17)$$

By examining the back emf and current waveform for a particular machine type, the factors,  $K_i$  and  $K_p$  in the sizing equation can be determined. Several typical waveforms and their corresponding  $K_i$  and  $K_p$ , repeated from Ref. [4], are shown in Table I.

### III. APPLICATION OF GENERAL PURPOSE SIZING EQUATION TO TFCCPM MACHINES

The concept of the transverse flux circumferential current type permanent magnet (TFCCPM) machine has been presented in Ref. [3]. A simplified representation of the TFCCPM topology is shown on Fig. 2. The outer diameter of this machine is given by

$$D_o = D_{go} + 2(d_{sso} + d_{cso}) \quad (18)$$

The diameter of the outer air-gap surface is

$$D_{go} = D_g + H_{PM} + 2g \quad (19)$$

where  $g$  is the length of the air-gap. Ref. [6] offers the following equation for estimating the air-gap

$$g = 4.7 \times 10^{-3} p^{-0.5} D_g \quad (20)$$

The radial height of the permanent magnet in the rotor  $H_{PM}$  depends on the flux focusing factor  $K_{focus}$  and pole pairs by

$$H_{PM} = \frac{\pi D_g K_{focus}}{8 p K_d} \quad (21)$$

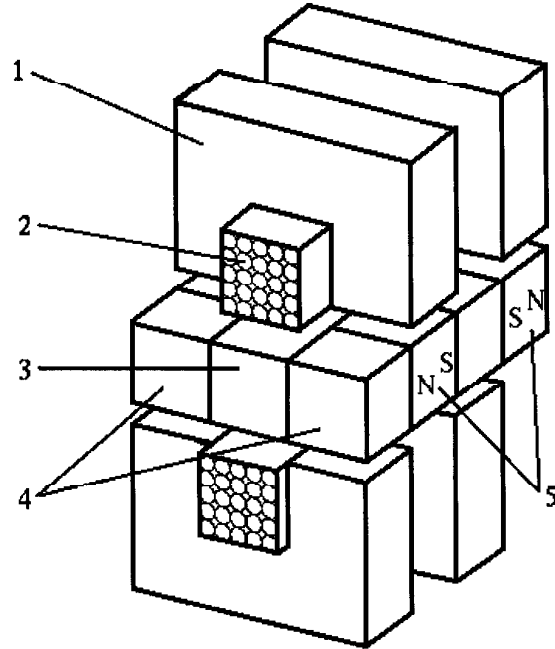
where  $K_d$  is the flux leakage factor of the PM machine obtained through a finite element study or through design experience. The most notable feature of this machine is that the factor  $K_{focus}$  can be readily adjusted by changing the radial height of the rotor to obtain the desired flux density in the air-gap. The topology results in a concept for flux-focusing structure that is very suitable for ferrite magnets.

The depth of the outer stator slot  $d_{sso}$  can be calculated as

$$d_{sso} = \frac{A_s}{2 J_s K_{cu} K_s} \quad (22)$$

where  $K_s$  is the ratio of the axial length of stator slot  $L_{ss}$  vs. the effective length of the machine  $L_e$ . The depth of the outer stator core  $d_{cso}$  is expressed as

$$d_{cso} = \frac{(1 - K_s) L_e B_g}{2 B_{cs}} \quad (23)$$



1. Stator soft iron 2. Ring winding 3. Rotor fiber ring  
4. Rotor soft iron 5. Permanent magnet

Fig. 2 Transverse Flux Circumferential Current PM (TFCCPM) Machine

Referring to Eq. (14) the ratio  $\lambda_o$  can be derived as

$$\lambda_o = \left(1 + \frac{\pi K_{focus}}{8 p K_d} + 9.4 \times 10^{-3} p^{-0.5} + \frac{A_s}{D_g J_s K_{cu} K_s} + (1 - K_s) K_L \left(\frac{B_g}{B_{cs}}\right)^{-1}\right) \quad (24)$$

From Eq. (24), it can be noted that the ratio  $\lambda_o$  not only depends upon the electrical loading  $A_s$  and the current density  $J_s$ , but also upon the distribution of flux density over the different portions of the machine. Due to the doubly salient structure, the flux densities in the stator core ( $B_{cs}$ ), the air gap ( $B_g$ ), and the rotor core ( $B_{cr}$ ) have essentially the same value. The choice of the flux density in the stator core can be estimated by [4]

$$B_{cs} = \begin{cases} 5.47 f^{-0.32} & f > 40 \text{ Hz} \\ 1.7 \text{ to } 1.8 & f \leq 40 \text{ Hz} \end{cases} \quad (25)$$

The air-gap flux density  $B_g$  can also be expressed as

$$B_g = K_{focus} B_{cs} \quad (26)$$

The flux focusing factor  $K_{focus}$  is related to the details of the structure of the permanent magnet machine. Generally [4]

$$K_{focus} = \frac{A_{pm}}{A_p} K_d \quad (27)$$

where  $A_{pm}$  is the surface area of permanent magnets,  $A_p$  is surface area of working pole per phase.

For the TFCCPM topology (Fig. 2), it can be determined that the emf factor for this machine is  $K_e = p\pi(1-K_s)/2$ , the number of phases of the machine  $m = 2$ . Because there is no rotor winding  $K_\phi = 0$ . Considering the trapezoidal waveforms in Table I (row 4), it can be determined that  $K_i K_p = 0.881$ . From Eq. (15), the following TFCCPM machine sizing equation is then obtained in which all units are SI,

$$P_{R(TFCCPM)} = 0.441 \pi(1-K_s) K_L \eta B_g A f \lambda_0 D_o^2 L_e \quad (28)$$

The power density of the TFCCPM machine is consequently,

$$\xi_{(TFCCPM)} = 1.762 (1-K_s) K_L \eta B_g A f \lambda_0 \quad (29)$$

In Eqs. (28) and (29), the only independent terms existing are  $K_L$  and  $K_s$  while the other terms either depend on  $K_L$  or  $K_s$ , or have certain physical limitations.

The optimal values of the ratio  $K_L$  and  $K_s$  were given considering power density and efficiency. A more detailed

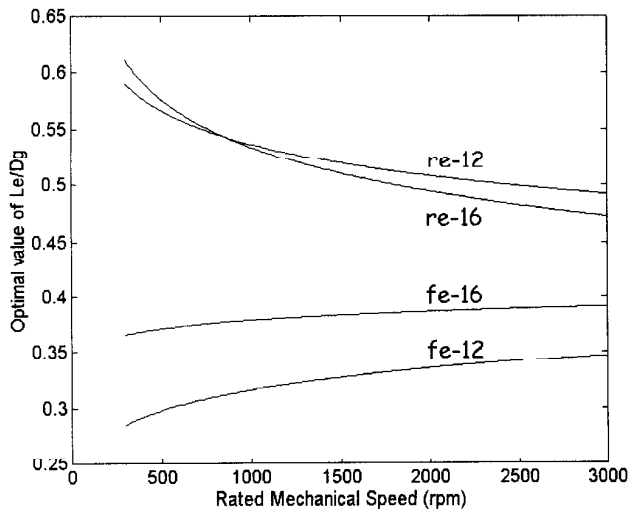


Fig. 3 Optimal value of  $K_L$  of the TFCCPM machine vs. rated mechanical speed  $n_s$  with different pole pairs  $p$  for maximum power density.

$$A=60 \text{ kA/m}, J_s=6.2 \times 10^6 \text{ A/m}^2, P_R=75 \text{ kw}, \\ p=6 \text{ (fe-12) and } p=8 \text{ (fe-16) using ferrite PM.}$$

$p=6$  (re-12) and  $p=8$  (re-16) using rare earth PM.

investigation using numerous candidate machine designs indicates that an optimal value of  $K_s$  is about 1/6 for a practical design, while the optimal value of  $K_L$  has a close connection with the rated mechanical speed  $n_s$ . Under a given electrical loading  $A$ , current density  $J_s$ , and the rated output power  $P_R$ , a group of curves can be generated which indicate the relationships between the optimal value of  $K_L$  and the rated mechanical speed  $n_s$  for different pole pairs  $p$  (Fig. 3). From this data, through power regression, it is possible to obtain the following expression,

$$\frac{L_e}{D_g} = \begin{cases} 0.1770 n_s^{0.0838} & p=6 \\ 0.3087 n_s^{0.0295} & p=8 \end{cases} \quad \text{Ferrite Magnets} \\ \begin{cases} 0.9276 n_s^{-0.0792} & p=6 \\ 1.1545 n_s^{-0.1116} & p=8 \end{cases} \quad \text{Rare-earth Magnets} \quad (30)$$

#### IV. COMPARISON BETWEEN INDUCTION AND TFCCPM MACHINES

It is now possible to compare the power densities of transverse flux (TFCCPM) machines through the use of the sizing and power density equations that have been derived. Because the squirrel cage induction machine is regarded as the "workhorse" of the ac machine family it can be considered as a "point of reference" for the other machines.

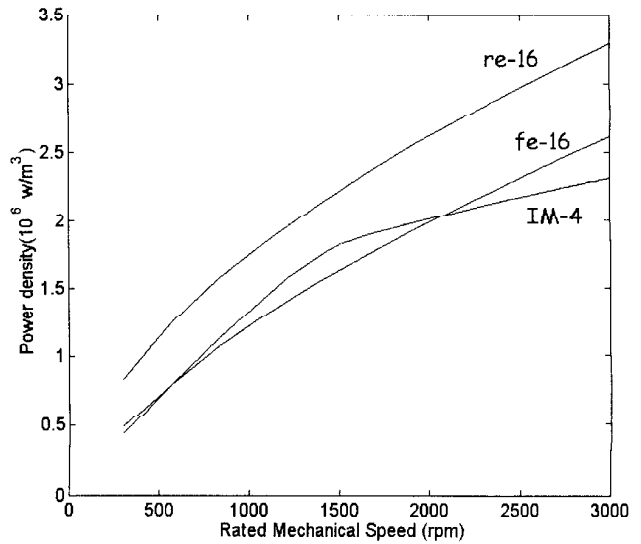


Fig. 4 Power densities of four pole induction machine and TFCCPM machines ( $A = 60kA/m$ ,  $J_s = 6.2 \times 10^6 A/m^2$ ,  $P_R = 75 kw$ ).

Fig. 4 shows a comparison of power densities among the 4-pole induction machines (IM-4) (Ref.[4]), the 16-pole TFCCPM machines with ferrite magnet (fe-16) and the 16-pole TFCCPM machines with rare earth magnet (re-16). Note that with the transverse principle a power density improvement of nearly a factor of two can be achieved for low speed machines if rare earth magnets are used. Although machines with rare earth magnets can achieve higher power density, further study has verified that the application of ferrite magnets to this structure is much more economical as might be expected. Thus, the proper material should again be chosen according to the purpose intended.

#### V. THE MAJOR DIFFERENCE BETWEEN TRANSVERSE FLUX TFCCPM MACHINES AND TRADITIONAL MACHINES

In the traditional electrical machines, one coil of the winding normally links the flux of one pole. If the pole number of the machine doubled, the flux linked by each coil decreases to half, also, the turns of each coil has to decreased to half due to the limit of the slot area. Although the total number of coils doubles, the total peak flux linkage of the winding decreases to one-half. Hence, if the machine operates at the same speed, the back-emf remains unchanged.

To make this point clear, the following approach can be outlined. For machine 1, the pole number is  $p_1$ , the total turns of one phase is  $N$ , the peak flux linked by one coil is  $\phi_1$ , the rated speed is  $\omega$ , the current rating is  $I$ . The average power output of one phase then is

$$P_1 = E_1 \cdot I = \frac{d\Lambda}{dt} \cdot I = \omega N \frac{d\phi_1}{d\theta} \cdot I = \omega N \frac{\phi_1}{2\pi} \cdot I = \omega N \frac{p_1 \phi_1}{2\pi} \cdot I$$

$p_1$

For machine 2, if the current rating and machine size remain unchanged, and the pole number is doubled ( $p_2=2p_1$ ), the flux linked by one coil must decrease to one-half ( $\phi_2= \phi_1/2$ ), the turns per coil has to decreased to one-half due to the limit of the slot size. Even though the number of coils has doubled, the total turns per phase still remains the same ( $N$ ). Hence,

$$P_2 = E_2 \cdot I = \omega N \frac{\phi_2}{2\pi} \cdot I = \omega N \frac{p_2 \phi_2}{2\pi} \cdot I = \omega N \frac{p_1 \phi_1}{2\pi} \cdot I = P_1$$

$p_2$

It is thus clear that the power rating of the machine remains the same even when the pole number has doubled.

Unlike the traditional electrical machines, the TFCCPM machine appears to belong to another family of machines--

circumferential current machines in which the coil of the winding links all the flux of the machine rather than the flux of one pole. Hence, when the pole number of the machine changes, the peak flux linkage of the winding does not change if leakage flux is neglected. A similar comparison between two machines of different pole number can be made.

Machine 1:

$$P_1 = E_1 \cdot I = \frac{d\Lambda}{dt} \cdot I = \omega N \frac{d\phi_1}{d\theta} \cdot I = \omega N \frac{\phi_1}{\frac{2\pi}{p_1}} \cdot I = \omega N \frac{p_1 \phi_1}{2\pi} \cdot I$$

Machine 2

$$P_2 = E_2 \cdot I = \omega N \frac{\phi_2}{\frac{2\pi}{p_2}} \cdot I = \omega N \frac{p_2 \phi_2}{2\pi} \cdot I = \omega N \frac{2 p_1 \phi_1}{2\pi} \cdot I = 2 P_1$$

$p_2$

Hence, the power of circumferential machine increases as its pole number increase even when the rated speed remains the same.

The same principle can also be found in the sizing equations. For traditional machine, the power density is proportional to  $f/p$  as shown in Eq. (1), while for TFCCPM machine, as shown in Eq. (28), the power density is proportional to  $f$ . Hence, the power density ratio  $\xi_{TFCCPM} / \xi_{IM}$  then is proportional to the pole number  $p$ . If a TFCCPM machine and an induction machine are compared at the same rated speed, the transverse flux machine will have higher power density when its pole number becomes greater than a certain threshold value. In this paper, it is found that this value is roughly 16 for machines with a medium power rating (75 KW). For different power ratings, this number may vary and can also be found with the same sizing equation approach outlined in this paper.

#### VI. CONCLUSION

In this paper, the following results have been obtained:

1. A detailed approach has been outlined to realize specific sizing and power density equations for the transverse flux machine by application of the general-purpose sizing and power density equations previously developed [4,5]. By defining suitable ratios and by considering the duality between transverse and radial flux machines, the sizing equations for the transverse flux machine takes a similar form to the general purpose sizing equations of radial flux machines. These equations permit a direct comparison of the capability of two basically different machine topologies based upon their overall occupied volume.

2. It has been shown that optimization of the aspect ratio  $K_L$  will achieve a maximum power density design and produce also machine with nearly the highest efficiency. In

comparison with traditional optimization methods, optimization based on the sizing equation using the outer diameter is shown to have a greater benefit, especially for the comparison of transverse flux machines with machines of traditional design.

3. The optimal value of  $K_L$  depends upon electrical loading, flux density, frequency, permanent magnet materials, and machine topology etc. However, further study shows it is more dependent on machine permanent magnet materials more than other factors. Hence, for a given machine and choice of PM, the optimal value of  $K_L$  varies over a relatively small range. For example, in fe-16 machine, the optimal  $K_L$  is between 0.365 to 0.40. On the other hand, different permanent magnet materials will result in a largely different range of the optimal  $K_L$ . For example, for the re-16 machine, the range is 0.435 to 0.61.

4. It is shown in the paper that the transverse flux circumferential machines have higher power density than the traditional induction machine over a wide range of rated speeds. In particular, when the rare earth magnet is applied the improvement can reach by over two times. Even when the ferrite magnet is used for low cost, the power density can still be improved at low speed.

## REFERENCES

- [1] T. A. Lipo and Yue Li, "CFMs - A New Family of Electrical Machines", IPEC'95, Japan, April 3-7, 1995, pp. 1-8.
- [2] T. A. Lipo and F. X. Wang, "Design and Performance of Converter Optimized AC Machines", IEEE Trans. on Industry Applications, vol. IA-20, No. 4 July/August 1984, pp. 834-844.
- [3] H. Weh, "On the Development of Inverter Fed Reluctance Machines for High Power Densities and High Outputs", etz Archiv, Bd. 6, 1984, pp. 135-144 (In German).
- [4] S. Huang, J. Luo, F. Leonardi, and T. A. Lipo, "A General Approach to Sizing and Power Density Equations for Comparison of Electrical Machines", IEEE -IAS Annual Meeting, Oct. 1996, pp. 836-842.
- [5] S. Huang, J. Luo, F. Leonardi, and T. A. Lipo, "A Comparison of Power Density for Axial Flux Machines Based on General Purpose Sizing Equations", IEEE Power Engineering Transaction. (accepted)
- [6] E. Levi, "Polyphase Motors -- A Direct Approach to Their Design", John Wiley and Sons, Inc., New York, 1984.